Differential Sensitivity of the Cystic Fibrosis (CF)-associated Mutants G551D and G1349D to Potentiators of the Cystic Fibrosis Transmembrane Conductance Regulator (CFTR) Cl− Channel*

Zhiwei Cai[‡], Alessandro Taddei[§], and David N. Sheppard[‡1]

From the [‡]Department of Physiology, University of Bristol, School of Medical Sciences, University Walk, Bristol BS8 1TD, United Kingdom and the [§]Laboratorio Genetica Molecolare, Istituto Giannina Gaslini, 16148 Genova, Italy

The genetic disease cystic fibrosis (CF) is caused by loss of function of the cystic fibrosis transmembrane conductance regulator (CFTR) Cl− channel. Two CF mutants, G551D and G1349D, affect equivalent residues in the highly conserved LSGGQ motifs that are essential components of the ATP-binding sites of CFTR. Both mutants severely disrupt CFTR channel gating by decreasing mean burst duration (MBD) and prolonging greatly the interburst interval (IBI). To identify small molecules that rescue the gating defects of G551D- and G1349D-CFTR and understand better how these agents work, we used the patch clamp technique to study the effects on G551D- and G1349D-CFTR of phloxine B, pyrophosphate (PP$_i$), and 2′-deoxy ATP (2′-dATP), three agents that strongly enhance CFTR channel gating. Phloxine B (5 μM) potentiated robustly G551D-CFTR Cl− channels by altering both MBD and IBI. In contrast, phloxine B (5 μM) decreased the IBI of G1349D-CFTR, but this effect was insufficient to rescue G1349D-CFTR channel gating. PP$_i$ (5 mM) potentiated weakly G551D-CFTR and was without effect on the G1349D-CFTR Cl− channel. However, by altering both MBD and IBI, albeit with different efficacies, 2′-dATP (1 mM) potentiated both G551D- and G1349D-CFTR Cl− channels. Using the ATP-driven nucleotide-binding domain dimerization model of CFTR channel gating, we suggest that phloxine B, PP$_i$ and 2′-dATP alter channel gating by distinct mechanisms. We conclude that G551D- and G1349D-CFTR have distinct pharmacological profiles and speculate that drug therapy for CF is likely to be mutation-specific.

The cystic fibrosis transmembrane conductance regulator (CFTR[2] (1)) is a unique member of the ATP-binding cassette transporter superfamily that plays a critical role in fluid and electrolyte transport across epithelia (2). CFTR is composed of two membrane-spanning domain (MSD) nucleotide-binding domain (NBD) motifs linked by a unique regulatory (R) domain. The membrane-spanning domains assemble to form a transmembrane pore with deep intracellular and shallow extracellular vestibules that funnel anions toward a selectivity filter, which determines the permeation properties of CFTR (3). Anion flow through the CFTR pore is controlled by cycles of ATP binding and hydrolysis at two ATP-binding sites located at the interface of the two NBDs (4). Stable ATP binding occurs at one ATP-binding site (site 1; formed by the Walker A and B motifs of NBD1 and the LSGGQ motif of NBD2), whereas rapid ATP turnover occurs at the other ATP-binding site (site 2; formed by the Walker A and B motifs of NBD2 and the LSGGQ motif of NBD1) (5, 6). The R domain contains multiple consensus phosphorylation sites on the surface of an unstructured domain (7). Phosphorylation of the R domain stimulates CFTR function by enhancing ATP-dependent channel gating at the NBDs (3). Thus, CFTR is an anion channel with exquisite regulation.

The importance of CFTR for transepithelial ion transport is dramatically highlighted by its malfunction in human disease. The genetic disease CF is caused by mutations that abolish the function of CFTR (2). Other diseases, such as autosomal dominant polycystic kidney disease and secretory diarrhea, involve inappropriate activity of CFTR (8, 9). In the search for rational new therapies for diseases caused by CFTR malfunction, a variety of agents have been identified that interact directly with CFTR. Agents that rescue the cell surface expression of CFTR (CFTR correctors) and/or potentiate channel activity (CFTR potentiators) might be used to treat CF. In contrast, agents that inhibit channel activity by pore occlusion or allosteric mechanisms might be used to treat autosomal dominant polycystic kidney disease and secretory diarrhea (10).

With ∼1,400 unique disease-causing mutations identified in the CFTR gene (the Cystic Fibrosis Mutation Database), a crucial issue for therapy development is the specificity of different drugs. For example, will one CFTR potentiator rescue all CF mutants that disrupt CFTR channel gating, or will specific CFTR potentiators need to be tailored to individual CF mutants? To explore the mutation specificity of CFTR potentiators and to understand better their mechanism of action, the aim of the present study was to investigate the effects of the CFTR potentiators phloxine B, pyrophosphate (PP$_i$), and 2′-deoxy-ATP (2′-dATP) on the CF mutants G551D and G1349D. We chose phloxine B, PP$_i$, and 2′-dATP because these agents robustly potentiate the gating behavior of wild-type human CFTR (11–14). Conversely, we selected the CF mutants G551D and G1349D because these mutants profoundly disrupt channel gating by affecting equivalent residues in the LSGGQ motifs of the two ATP-binding sites of CFTR (G551D, site 2, and G1349D, site 1) (4–6; 15–19) and because G551D is a common CF mutation (2). To quantify the efficacy with which the different CFTR potentiators restore normal channel gating to G551D- and G1349D-CFTR, we employed high resolution single-channel recording and

kinetic analyses of channel gating. Then using the ATP-driven NBD dimerization model of CFTR channel gating (5, 20), we explain how the different CFTR potentiators alter CFTR channel gating.

MATERIALS AND METHODS

Cells and Cell Culture—For this study, we used mouse mammary epithelial cells (C127 cells) stably expressing either wild-type human CFTR or the CF mutant G1349D and Fischer rat thyroid (FRT) epithelial cells stably expressing the CF mutant G551D.[3] C127 cells were generous gifts of Professor M. J. Welsh (University of Iowa, Iowa City, IA) and Dr C. R. O'Riordan (Genzyme, Framingham, MA), whereas FRT cells were a generous gift of Drs. L. J. V. Galietta and O. Zegarra-Moran (Istituto Giannina Gaslini, Genoa, Italy). C127 and FRT cells were cultured and used as described previously (21, 22).

Electrophysiology—CFTR Cl⁻ channels were recorded in excised inside-out membrane patches using an Axopatch 200A patch clamp amplifier (Axon Instruments Inc., Union City, CA) and pCLAMP data acquisition and analysis software (version 6.03, Axon Instruments Inc.) as described previously (21, 23). The established sign convention was used throughout; currents produced by positive charge moving from intra- to extracellular solutions (anions moving in the opposite direction) are shown as positive currents.

The pipette (extracellular) solution contained (in mM): 140 N-methyl-D-glucamine, 140 aspartic acid, 5 $CaCl_2$, 2 $MgSO_4$, and 10 TES, adjusted to pH 7.3 with Tris ([Cl^-], 10 mM). The bath (intracellular) solution contained (in mM): 140 N-methyl-D-glucamine, 3 $MgCl_2$, 1 Cs-EGTA, and 10 TES, adjusted to pH 7.3 with HCl ([Cl^-], 147 mM; free [Ca^{2+}], $<10^{-8}$ M) and was maintained at 37 °C using a temperature-controlled microscope stage (Brook Industries, Lake Villa, IL).

After excision of inside-out membrane patches, we added the catalytic subunit of PKA (75 nM) and ATP (1 mM) to the intracellular solution within 5 min of patch excision to activate CFTR Cl⁻ channels. To prevent channel rundown in excised membrane patches, we added PKA to all intracellular solutions, maintained the ATP concentration at 1 mM, and clamped voltage at −50 mV. Under these conditions, CFTR rundown in excised membrane patches from either C127 or FRT cells is minimal (21).[4] With the exception of 2'-dATP, which replaced ATP in the intracellular solution, the effects of CFTR potentiators on wild-type and mutant CFTRs were tested by adding agents to the intracellular solution in the continuous presence of ATP (1 mM) and PKA (75 nM). Because the effects of phloxine B on the CFTR Cl⁻ channel are only partially reversible (11), specific interventions were not bracketed by control periods made with the same concentrations of ATP and PKA but without the test agent.

To determine the relationship between phloxine B concentration and channel activity for G551D- and G1349D-CFTR, we used membrane patches containing multiple active channels. For all other studies, we used membrane patches containing small numbers of active channels (wild-type and G1349D-CFTR, ≤4; G551D-CFTR, ≤6). We determined the number of channels in a membrane patch from the maximum number of simultaneous channel openings observed during the course of an experiment. To minimize errors when counting the number of active channels, we employed two strategies. First, we recorded channel activity for prolonged periods (30–60 min) and verified that recordings were of sufficient length to ascertain the correct number of active channels (24, 25). Second, we used experimental conditions that robustly potentiate channel activity to determine the number of active channels in a membrane patch. For wild-type and G1349D-CFTR Cl⁻ channels, channel numbers were counted in the presence of ATP (1 mM) and PKA (75 nM) alone. In contrast, the presence of the CFTR potentiators phloxine B or 2'-dATP were required to determine the number of G551D-CFTR Cl⁻ channels in a membrane patch. Despite our precautions, we cannot exclude the possibility of unobserved G551D- and G1349D-CFTR Cl⁻ channels in membrane patches. Therefore, values of P_o for G551D- and G1349D-CFTR might possibly be overestimated.

CFTR Cl⁻ currents were initially recorded on digital audio tape using a digital tape recorder (Biologic Scientific Instruments, model DTR-1204; Intracel Ltd., Royston, UK) at a bandwidth of 10 kHz. On playback, records were filtered with an eight-pole Bessel filter (Frequency Devices™, model 902LPF2; SCENSYS Ltd., Aylesbury, UK) at a corner frequency of 500 Hz and acquired using a Digidata 1200 interface (Axon Instruments, Inc.) and pCLAMP at a sampling rate of 5 kHz. For the purpose of illustration, single-channel records were filtered at 500 Hz and digitized at 1 kHz.

For concentration-response studies, average current (I) for a specific intervention was determined as the average of all the data points collected during the intervention. To plot the relationship between drug concentration and CFTR Cl⁻ current, current values were expressed as a percentage of the control CFTR Cl⁻ current recorded in the presence of ATP (1 mM) and PKA (75 nM) but in the absence of drug. To measure single-channel current amplitude (i), Gaussian distributions were fit to current amplitude histograms.

nP_o was calculated by dividing I by i. For P_o and burst analyses, lists of open and closed times were created and analyzed as described previously (26). Burst analysis was performed as described by Carson *et al.* (27), using a t_c (the time that separates interburst closures from intraburst closures) of 15 ms. The mean interburst interval (T_{IBI}) was calculated by using the equation (28)

$$P_o = T_b/(T_{MBD} + T_{IBI}) \qquad \text{(Eq. 1)}$$

where T_b = (mean burst duration) × (open probability within a burst). Mean burst duration (T_{MBD}) and open probability within a burst ($P_{o\ (burst)}$) were determined directly from experimental data using pCLAMP software. P_o was calculated from either open- and closed-times, as described previously (26), or by using the equation:

$$P_o = I/(n \times i) \qquad \text{(Eq. 2)}$$

where n represents the number of active channels in the membrane patch. For wild-type CFTR, only membrane patches that contained a single active channel were used for burst analysis, whereas for G551D- and G1349D-CFTRs, we used membrane patches containing no more than four active channels. As described by Carson *et al.* (27), we analyzed only bursts of single-channel openings with no super imposed openings that were separated from one another by a minimum of 15 ms. Similar values of MBD and IBI were acquired using membrane patches containing either one or between two and four active channels. For example, for G1349D-CFTR, when $n = 1$, MBD = 34.4 ± 7.8 ms and IBI = 3,873 ± 1,239 ms ($n = 5$), and when $n = 2–4$, MBD = 36.8 ± 6.5 ms

---

[3] To verify that the single-channel behavior of CFTR in FRT and C127 cells is equivalent, we measured i, P_o, and the response to phloxine B of CFTR Cl⁻ channels in excised inside-out membrane patches clamped at −50 mV using solutions identical to those employed in the present study with the exception that Bis-Tris (5 mM) + Trizma (Tris base) (5 mM) replaced TES (10 mM) in the intracellular solution to which was added ATP (1 mM) and PKA (75 nM). Neither i (C127 cells, −0.88 ± 0.06 pA ($n = 18$); FRT cells, −0.86 ± 0.03 pA ($n = 4$); $p = 0.64$) nor P_o (C127 cells, 0.52 ± 0.04 ($n = 18$); FRT cells, 0.50 ± 0.05 ($n = 4$); $p = 0.40$) differed between the two cell lines (J.-H. Chen, Z. Cai, and D. N. Sheppard, unpublished data). Similarly, the response of wild-type CFTR to phloxine B was equivalent in the two cell lines (C127, Fig. 2B; FRT, $n = 3$ (Z. Cai and D. N. Sheppard, unpublished data)).

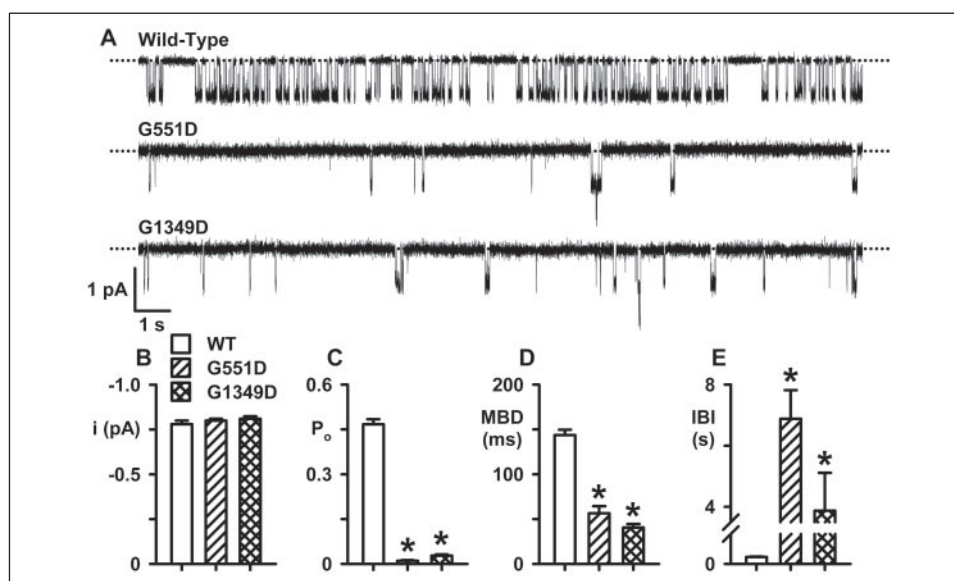[4] Z. Cai, J.-H. Chen, and D. N. Sheppard, data not shown

FIGURE 1. **The single-channel activity of wild-type (*WT*), G551D- and G1349D-CFTRs.** *A*, representative single-channel recordings of wild-type, G551D-, and G1349D-CFTRs in excised inside-out membrane patches from C127 cells expressing wild-type and G1349D-CFTR and FRT cells expressing G551D-CFTR. In this and subsequent figures, unless otherwise indicated, ATP (1 mM) and PKA (75 nM) were continuously present in the intracellular solution, voltage was −50 mV, and there was a large Cl^- concentration gradient across the membrane patch (internal $[Cl^-] = 147$ mM; external $[Cl^-] = 10$ mM). The *dotted lines* indicate where channels are closed, and downward deflections of the traces correspond to channel openings. For wild-type and G1349D-CFTRs, the membrane patches contained one and two active channels, respectively. For G551D-CFTR, four active channels were observed when phloxine B (5 μM) was added to the intracellular solution (not shown). *B–E, i, P_o*, MBD, and IBI of wild-type, G551D-, and G1349D-CFTRs. *Columns* and *error bars* indicate means + S.E. (wild-type, $n = 20$ for P_o and i, $n = 10$ for MBD and IBI; G551D, $n = 35$ for i, $n = 10$ for P_o, MBD, and IBI; G1349D, $n = 25$ for i, P_o, and MBD but $n = 5$ for IBI). The *asterisks* indicate values that are significantly different from those of wild-type CFTR ($p < 0.01$). Other details are as under "Materials and Methods."

and IBI = 2,090 ± 481 ms ($n = 12$) ($p > 0.1$ for both sets of data). Comparable values of MBD were also obtained using a t_c of 30 ms.[5]

To perform maximum likelihood analysis and develop kinetic models of CFTR channel gating, we used the QuB software suite as described previously (11, 29). For consistency with analyses using pCLAMP software, transitions <1 ms were excluded. Only membrane patches that contained a single active channel were used for maximum likelihood analysis and kinetic modeling.

Reagents—PKA was purchased from Promega Corp. (Southampton, UK). ATP (disodium salt), 2′-deoxyadenosine 5′-triphosphate disodium salt (2′-dATP), phloxine B (2′,4′,5′,7′-tetrabromo-4,5,6,7-tetrachlorofluorescein), PP_i (tetrasodium salt), and TES were obtained from Sigma. All other chemicals were of reagent grade.

Stock solutions of phloxine B were prepared in Me_2SO and stored at −20 °C. Immediately before use, stock solutions were diluted to achieve final concentrations. Me_2SO did not affect the activity of CFTR (21). Stock solutions of PP_i were prepared as described by Carson *et al.* (13), while those for ATP and 2′-dATP were prepared immediately before each experiment.

Statistics—Results are expressed as means ± S.E. of *n* observations. To compare sets of data, we used either Student's paired or unpaired *t* test. Differences were considered statistically significant when $p < 0.05$. All tests were performed using SigmaStat™ (version 2.03, Jandel Scientific GmbH, Erkrath, Germany).

RESULTS

The Single-channel Activity of Wild-type, G551D-, and G1349D-CFTRs—Before investigating the rescue of the CF mutants G551D and G1349D by CFTR potentiators, we quantified their single-channel activity. Fig. 1*A* shows representative single-channel recordings of wild-type, G551D-, and G1349D-CFTR. Like other NBD mutants (3), G551D- and G1349D-CFTR were without effect on *i* but perturbed

severely channel gating (Fig. 1, *A* and *B*). The gating behavior of wild-type CFTR is characterized by bursts of channel openings, interrupted by brief flickery closures and separated by longer closures between bursts. In contrast, G551D- and G1349D-CFTR both attenuated the duration of bursts and prolonged dramatically the interburst interval (Fig. 1*A*). As a result, the P_o of G551D- and G1349D-CFTR were reduced markedly when compared with that of wild-type CFTR (Fig. 1*C*).

To explain the marked differences in P_o between wild-type CFTR and the CF mutants, we performed an analysis of bursts. Based on analyses of closed-time histograms (wild-type CFTR, $\tau_c = 14.87 \pm 0.51$ ms ($n = 10$); G1349D-CFTR, $\tau_c = 17.41 \pm 1.49$ ms ($n = 5$); $p > 0.05$), we used a burst delimiter (τ_c) of 15 ms to discriminate inter- and intraburst closures.[6] The MBD of G551D- and G1349D-CFTR were similar and both about one-third that of wild-type CFTR (Fig. 1*D*). In contrast, the IBI of G551D- and G1349D-CFTR were prolonged strikingly when compared with that of wild-type CFTR (Fig. 1*E*).

Phloxine B Rescues the Gating Defect of G551D-CFTR but Not That of G1349D-CFTR—The fluorescein derivative phloxine B potentiates efficaciously wild-type and ΔF508-CFTR Cl^- currents (11). Like its effects on wild-type CFTR (11), phloxine B (0.1–5 μM) potentiated greatly G551D-CFTR Cl^- currents, whereas phloxine B (10–40 μM) inhibited channel activity (Fig. 2, *A* and *B*). Interestingly, for both wild-type and G551D-CFTR, phloxine B (5 μM) potentiated the maximum Cl^- current (Fig. 2*B*). However, because under control conditions the activity of G551D-CFTR is much lower than that of wild-type CFTR (Fig. 1), the potentiation of G551D-CFTR by phloxine B exceeded greatly that of wild-type CFTR (Fig. 2*B*).

Phloxine B potentiates wild-type CFTR Cl^- currents by prolonging MBD, and thus, increasing P_o (11). To determine how phloxine B poten-

---

[5] Z. Cai and D. N. Sheppard, data not shown.

[6] For G551D-CFTR, no membrane patches containing a single active CFTR Cl^- channel were obtained. However, given the very large difference in the duration of intra- and interburst closures for G551D-CFTR, misclassification errors when defining bursts should be rare.

FIGURE 2. **Phloxine B (*PB*) potentiates strongly the single-channel activity of G551D-CFTR.** *A*, representative recordings show the effects of phloxine B (1 and 5 μM) on the activity of G551D-CFTR Cl$^-$ channels. *B*, effects of phloxine B concentration on G551D (*filled circles* and *solid line*) and wild-type CFTR (*open circles* and *dotted line*). Data are means ± S.E. (G551D, $n = 5$–8; wild-type CFTR, $n = 4$–9) at each point. Values above the *dashed line* indicate CFTR potentiation, whereas values below the line indicate CFTR inhibition. *C*, effect of phloxine B concentration on *i* of G551D- (*filled circles* and *solid line*) and wild-type CFTR (*open circles* and *dotted line*). Data are means ± S.E. ($n = 5$–14) at each point. *D–F*, effects of phloxine B (5 μM) on P_o, MBD, and IBI of G551D-CFTR Cl$^-$ channels. *Columns* and *error bars* indicate means + S.E. ($n = 7$). The *asterisks* indicate values that are significantly different from the control values ($p < 0.05$). Other details are as under "Materials and Methods."
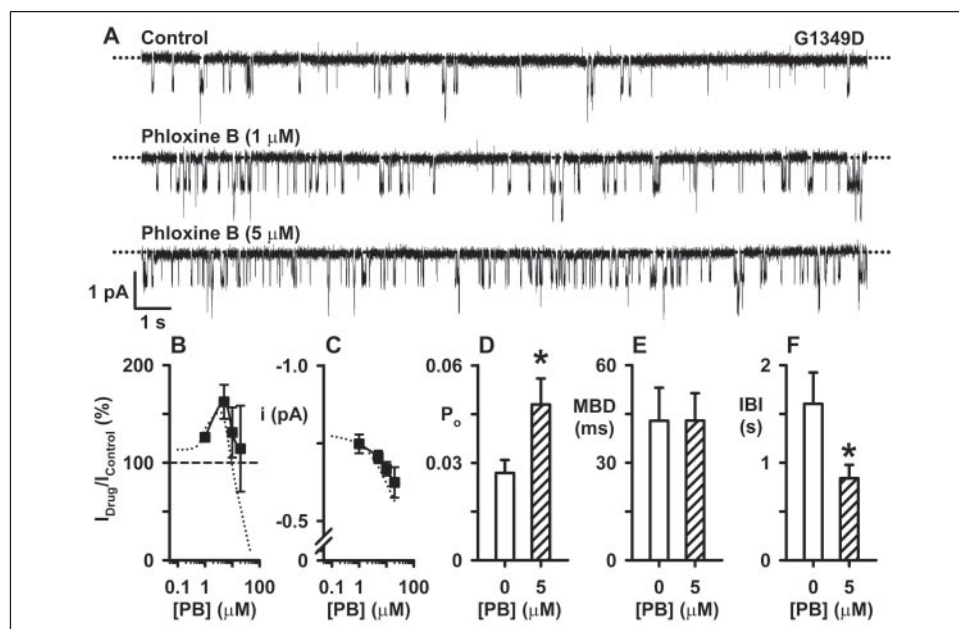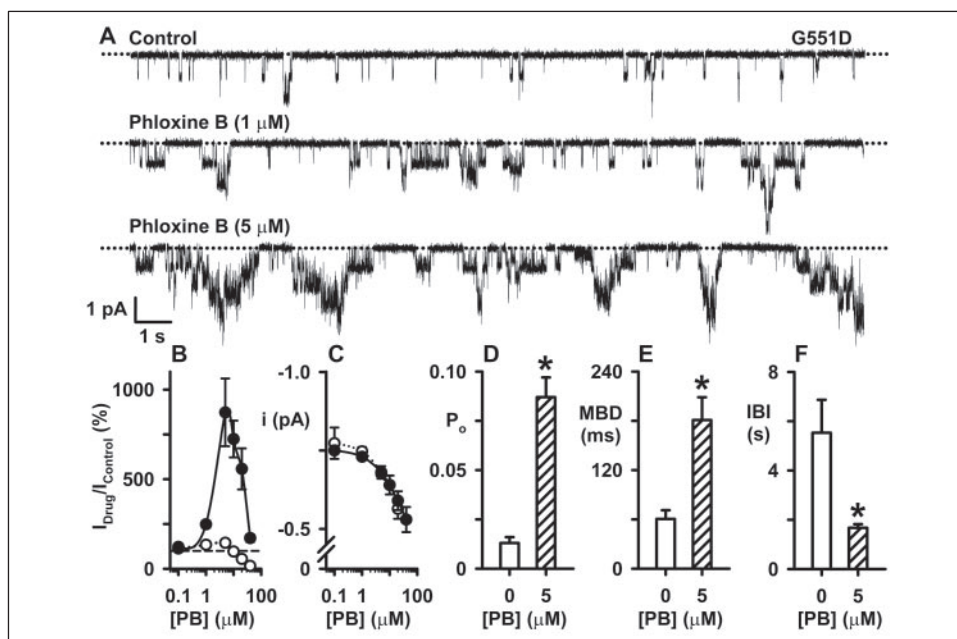

FIGURE 3. **Phloxine B potentiates weakly the single-channel activity of G1349D-CFTR.** *A*, representative recordings show the effects of phloxine B (1 and 5 μM) on the activity of G1349D-CFTR Cl$^-$ channels. *B*, effects of phloxine B concentration on G1349D-CFTR Cl$^-$ currents (*filled squares* and *solid line*). Data are means ± S.E. ($n = 5$–7) at each point. For comparison, the concentration-response relationship for wild-type CFTR is shown as a *dotted line*. *C*, effect of phloxine B concentration on *i* of G1349D- (*filled squares* and *solid line*) and wild-type CFTR (*dotted line*). Data are means ± S.E. ($n = 5$–8). *D–F*, effects of phloxine B (5 μM) on P_o, MBD, and IBI of G1349D-CFTR Cl$^-$ channels. *Columns* and *error bars* indicate means + S.E. ($n = 7$). The *asterisks* indicate values that are significantly different from the control values ($p < 0.05$). Other details are as described in the legend for Fig. 2.

tiates G551D-CFTR Cl$^-$ currents, we measured *i*, P_o, MBD, and IBI in the absence and presence of the drug. Phloxine B (0.1–40 μM) caused a concentration-dependent decrease in *i* equivalent to that observed with wild-type CFTR (Fig. 2*C*), suggesting that phloxine B does not potentiate G551D-CFTR by increasing current flow through the channel. Instead, phloxine B (1–5 μM) potentiated G551D-CFTR by enhancing dramatically channel gating, and thus, P_o (Fig. 2, *A* and *D*, $p < 0.01$). Moreover, as a result of the effects of the drug on channel gating, the number of active channels increased ($n = 7$; Fig. 2*A*). Importantly, phloxine B (5 μM) prolonged the MBD of G551D-CFTR Cl$^-$ channels to a length equivalent to that of wild-type CFTR in the absence of drugs (Figs. 1*D* and 2*E*; $p > 0.05$). However, although phloxine B (5 μM) decreased the IBI of G551D-CFTR by 62%, it was still over 11-fold longer than that of wild-type CFTR in the absence of the drug (Figs. 1*E* and 2*F*; $p < 0.001$).

Phloxine B (1–20 μM) also had biphasic effects on G1349D-CFTR Cl$^-$ currents with phloxine B (5 μM) potentiating the maximum current (Fig. 3, *A* and *B*) (11). Of note, the magnitude of G1349D-CFTR Cl$^-$ current potentiated by phloxine B (5 μM) was much smaller than that of G551D-CFTR but equivalent to that of wild-type CFTR (Figs. 2*B* and 3*B*). Because the single-channel activity of G1349D-CFTR is greatly diminished when compared with that of wild-type CFTR (Fig. 1), these results indicate that phloxine B fails to rescue the gating defect of G1349D-CFTR.

Phloxine B caused a concentration-dependent reduction in *i* (Fig. 3*C*) but no change in the number of active G1349D-CFTR Cl$^-$ channels ($n = 8$, Fig. 3*A*). Interestingly, G1349D-CFTR Cl$^-$ channels tended to open more frequently in the presence of phloxine B (Fig. 3*A*). For example, phloxine B (5 μM) caused a small but significant increase in P_o (Fig. 3*D*; $p < 0.05$) by reducing IBI 42% ($p < 0.05$) without altering MBD ($p > 0.05$; Fig. 3, *E* and *F*). However, the IBI of G1349D-CFTR in the presence

FIGURE 4. **Effects of PP_i on the single-channel activity of G551D-CFTR.** *A*, representative recordings show the effects of PP_i (5 mM) on the activity of G551D-CFTR Cl^- channels. *B–E*, effects of PP_i (5 mM) on i, P_o, MBD, and IBI of G551D-CFTR. *Columns* and *error bars* indicate means + S.E. ($n = 10$ for i, $n = 6$ for P_o, MBD, and IBI). The *asterisks* indicate values that are significantly different from the control value ($p < 0.05$). Increasing the PP_i concentration to 10 mM failed to enhance further the single-channel activity of G551D-CFTR (nP_o: control, 0.07 ± 0.03; PP_i (10 mM), 0.23 ± 0.10, $n = 6$; $p = 0.7$ *versus* PP_i (5 mM) data). Other details are as under "Materials and Methods."
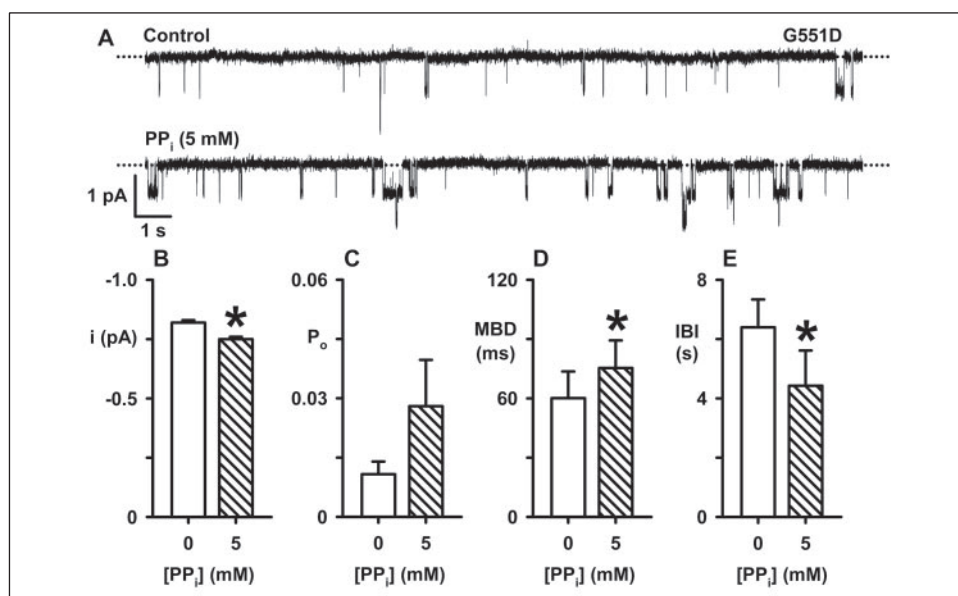
of phloxine B (5 μM) was over 5-fold longer than that of wild-type CFTR in the absence of drug. Thus, our data demonstrate that phloxine B rescues the gating defect of G551D-CFTR but not that of G1349D-CFTR.

Effects of PP_i on the Single-channel Activity of G551D- and G1349D-CFTR—The non-hydrolyzable inorganic phosphate analogue, PP_i, enhances robustly wild-type CFTR Cl^- currents by (i) increasing the rate of channel opening and (ii) decreasing markedly the rate of channel closure (12, 13). Fig. 4A demonstrates that PP_i (5 mM) augmented the single-channel activity of G551D-CFTR. However, the potentiation achieved by PP_i (5 mM) was much weaker than that of phloxine B (5 μM; Figs. 2A and 4A) and not increased at higher PP_i concentrations (as described in the legend for Fig. 4). PP_i (5 mM) caused a small but significant reduction in i (Fig. 4B) but was without effect on the number of active channels ($n = 10$; Fig. 4A). PP_i (5 mM) increased, but not significantly, the P_o of G551D-CFTR by enhancing slightly MBD and curtailing weakly IBI (Fig. 4, *C–E*).

Like phloxine B (5 μM), PP_i (5 mM) failed to potentiate the single-channel activity of G1349D-CFTR (Fig. 5). There was (i) a small decrease in i (Fig. 5B, $p < 0.05$), (ii) no change in the number of active channels ($n = 6$, Fig. 5A), (iii) no significant increase in P_o (Fig. 5C), (iv) no prolongation of MBD (Fig. 5D), and (v) a small, but not significant, decrease in IBI (Fig. 5E). Higher concentrations of PP_i (10 mM) were also ineffective ($n = 2$, data not shown).

2′-Deoxy-ATP Activates Both G551D- and G1349D-CFTR Cl^- Channels—Because both phloxine B and PP_i failed to potentiate G1349D-CFTR, we searched for other agents that might rescue this CF mutant. A particularly attractive candidate for study was the hydrolyzable ATP analogue 2′-dATP, which gates wild-type CFTR more effectively than ATP in planar lipid bilayers (14).

Fig. 6A demonstrates that substitution of ATP (1 mM) by 2′-dATP (1 mM) altered dramatically CFTR channel gating; the duration of bursts was prolonged greatly, and the interburst interval was diminished markedly. However, neither i nor the number of active channels changed following the substitution of ATP (1 mM) by 2′-dATP (1 mM; Fig. 6A). Fig. 6B quantifies the effects of 2′-dATP on i, P_o, MBD, and IBI. When compared with ATP (1 mM), 2′-dATP (1 mM) increased MBD by 84%, decreased IBI by 46%, and thus, increased P_o by 53% (Fig. 6B).

To understand better how 2′-dATP alters channel gating, we investigated the gating kinetics of wild-type CFTR using membrane patches that contained only a single active channel. Winter *et al.* (30) demonstrated previously that a linear three-state model is the simplest model to describe CFTR channel gating (Fig. 6C). In this model, C_1 represents the long duration closed state separating channel openings, and $C_2 \leftrightarrow O$ represents the bursting state in which channel openings (O) are interrupted by brief flickery closures (C_2). Transitions between the three states are described by the rate constants β_1, β_2, α_1, and α_2. Winter *et al.* (30) demonstrated that intracellular ATP regulates CFTR by accelerating the transition from C_1 to C_2.

The open- and closed-time histograms of wild-type CFTR are best fit by one- and two-component exponential functions in the presence of either ATP or 2′-dATP (*e.g.* Ref. 28 and data not shown). This suggests that the gating behavior of wild-type CFTR in the presence of 2′-dATP may be described by the $C_1 \leftrightarrow C_2 \leftrightarrow O$ kinetic scheme.[7] Fig. 6C shows the rate constants for the $C_1 \leftrightarrow C_2 \leftrightarrow O$ kinetic scheme calculated using QuB software (28, 29). When compared with the ATP data, β_1 was increased by 90%, α_1 was decreased by 27%, β_2 was increased by 12%, but α_2 was unchanged. The increase in β_1 shortened the interburst interval by accelerating the entry into the bursting state. In contrast, the decrease in α_1 increased the duration of bursts by slowing the exit from the bursting state. The small increase in β_2 further prolonged the duration of bursts. Thus, 2′-dATP enhanced CFTR channel gating by increasing both the frequency and the duration of bursts of channel openings.

Fig. 7A suggests that 2′-dATP (1 mM) enhanced markedly G551D-CFTR channel gating with the result that the number of active channels increased. Quantification of the effects of 2′-dATP on G551D-CFTR revealed (i) no significant change in i (Fig. 7B), (ii) a 10-fold increase in P_o (Fig. 7C), (iii) a 3.5-fold enhancement of MBD (Fig. 7D), and (iv) a 61% decrease in IBI (Fig. 7E). Of note, the MBD of G551D-CFTR in the presence of 2′-dATP (1 mM) was similar to that of wild-type CFTR in the presence of ATP (1 mM; Figs. 1D and 7D). However, the IBI of G551D-CFTR in the presence of 2′-dATP (1 mM) was over 17-fold longer than that of wild-type CFTR in the presence of ATP (1 mM; Figs. 1E and 7E).

Finally, we tested the effects of 2′-dATP on the single-channel activity of G1349D-CFTR. Replacement of ATP (1 mM) by 2′-dATP (1 mM) was with-

---

[7] Comparable results were observed using the $C_1 \leftrightarrow O \leftrightarrow C_2$ kinetic scheme (Ref. 28 and data not shown).

FIGURE 5. **Pyrophosphate (5 mM) fails to potentiate the single-channel activity of G1349D-CFTR.** *A*, representative recordings show the effects of PP_i (5 mM) on the activity of G1349D-CFTR Cl$^-$ channels. *B–E*, effects of PP_i (5 mM) on *i*, P_o, MBD, and IBI of G1349D-CFTR. *Columns* and *error bars* indicate means + S.E. (*n* = 6 for *i* and P_o, *n* = 5 for MBD and IBI).
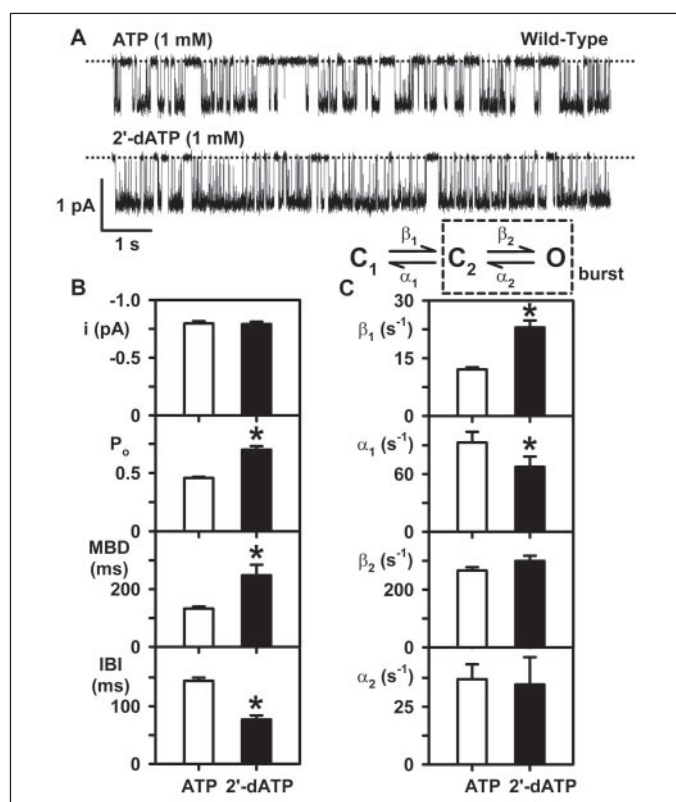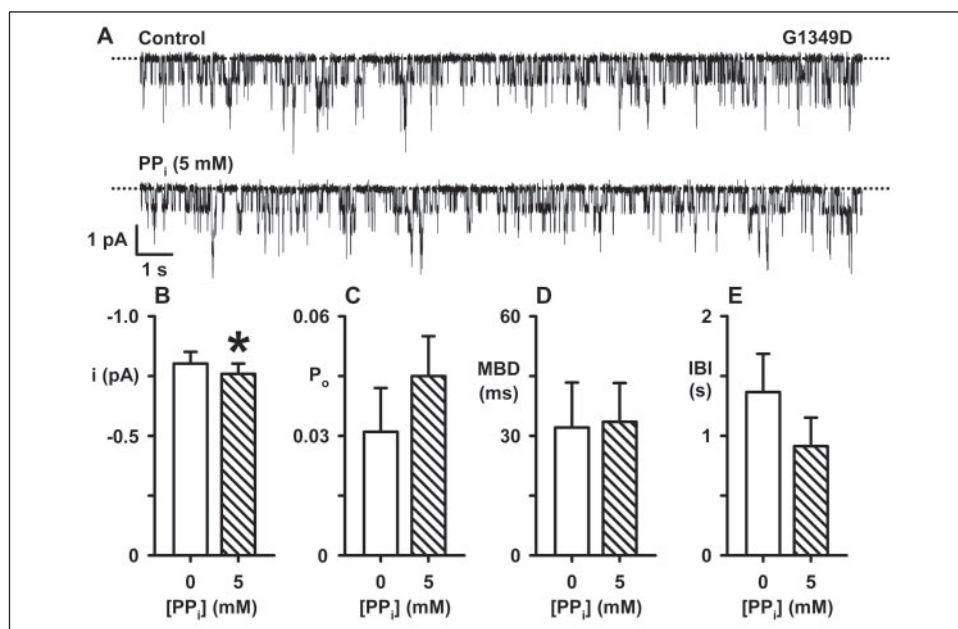

FIGURE 6. **2′-dATP potentiates strongly the single-channel activity of phosphorylated wild-type CFTR.** *A*, representative recordings show the activity of a single wild-type CFTR Cl$^-$ channel in the presence of either ATP (1 mM) or 2′-dATP (1 mM). PKA (75 nM) was continuously present in the intracellular solution. *B*, *i*, P_o, MBD, and IBI of wild-type CFTR in the presence of either ATP (1 mM) or 2′-dATP (1 mM). *Columns* and *error bars* are means + S.E. (*n* = 4–5). The *asterisks* indicate values that are significantly different from the ATP (1 mM) values (*p* < 0.05). *C*, rate constants of the $C_1 \leftrightarrow C_2 \leftrightarrow O$ kinetic scheme in the presence of either ATP (1 mM) or 2′-dATP (1 mM). A linear three-state model that describes the gating behavior of phosphorylated wild-type CFTR Cl$^-$ channels (30) is shown above the data. States C_1, C_2, and O represent two closed states and one open state, respectively, while β_1, β_2, α_1, and α_2 represent the rate constants describing transitions between the open and closed states. States enclosed within the *dashed box* represent the bursting state. *Columns* and *error bars* are means + S.E. (*n* = 4). The *asterisks* indicate values that are significantly different from the ATP (1 mM) values (*p* < 0.05).

out effect on *i* but augmented G1349D-CFTR channel gating, leading to an increase in the number of active channels (Fig. 8). In the presence of 2′-dATP (1 mM), the P_o and MBD of G1349D-CFTR increased 3.6- and 1.2-fold, respectively (Fig. 8, *C* and *D*), while IBI decreased by 54% (Fig. 8*E*). However, the MBD and IBI of G1349D-CFTR in the presence of 2′-dATP (1 mM) were 63% shorter and 2.6-fold longer, respectively, than those of wild-type CFTR in the presence of ATP (1 mM; Figs. 1, *D* and *E*, and 8, *D* and *E*). We interpret our data to suggest that 2′-dATP potentiates wild-type, G551D-, and G1349D-CFTR channel gating by similar mechanisms but that 2′-dATP incompletely restores normal channel gating to either G551D-CFTR or G1349D-CFTR.

DISCUSSION

The CF mutants G551D and G1349D affect equivalent residues in the LSGGQ motifs of NBD1 and NBD2. These mutants severely disrupt CFTR channel gating by slowing profoundly the rate of channel opening and accelerating markedly the rate of channel closure. The CFTR potentiators phloxine B and 2′-dATP, but not PP_i, augment G551D-CFTR channel gating, whereas only 2′-dATP enhances that of G1349D-CFTR. Our results demonstrate that G551D- and G1349D-CFTR have distinct pharmacological profiles.

Molecular Mechanisms of CFTR Dysfunction in CF

Previous studies demonstrated that G551D- and G1349D-CFTR cause a loss of Cl$^-$ channel function by disrupting ATP binding, hydrolysis, and thus, channel gating (17, 19, 31). Building on these data, our quantitative analysis of channel gating reveals that these mutants have exceptionally slow opening rates and very fast closing rates when compared with those of wild-type CFTR. To explain the severity of these gating defects, we consider how G551D- and G1349D-CFTR might perturb the ATP-driven NBD dimerization model of CFTR channel gating (5, 20).

The exceptionally slow rates of G551D- and G1349D-CFTR channel opening suggest that these mutants impede ATP binding to sites 1 and 2 with the result that the rate of NBD dimerization is retarded. Moreover, once the NBD dimer forms in G551D- and G1349D-CFTR Cl$^-$ channels, it is inherently unstable. Consequently, the rate of NBD dissociation is accelerated, and thus, the duration of channel openings is

FIGURE 7. **2'-dATP potentiates strongly G551D-CFTR Cl⁻ channels.** *A*, single-channel recordings of G551D-CFTR in the presence of either ATP (1 mM) or 2'-dATP (1 mM). PKA (75 nM) was continuously present in the intracellular solution. *B–E*, effects of 2'-dATP on i, P_o, MBD, and IBI of G551D-CFTR, respectively. *Columns* and *error bars* indicate means + S.E. ($n = 8$ for i, $n = 5$ for P_o, MBD, and IBI). The *asterisks* indicate values that are significantly different from the control values ($p < 0.05$).
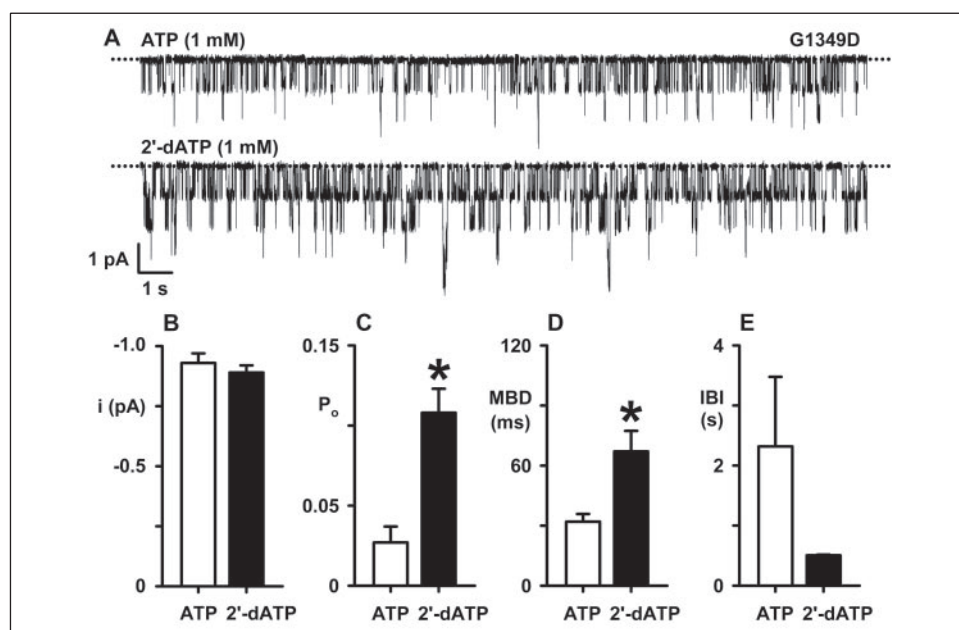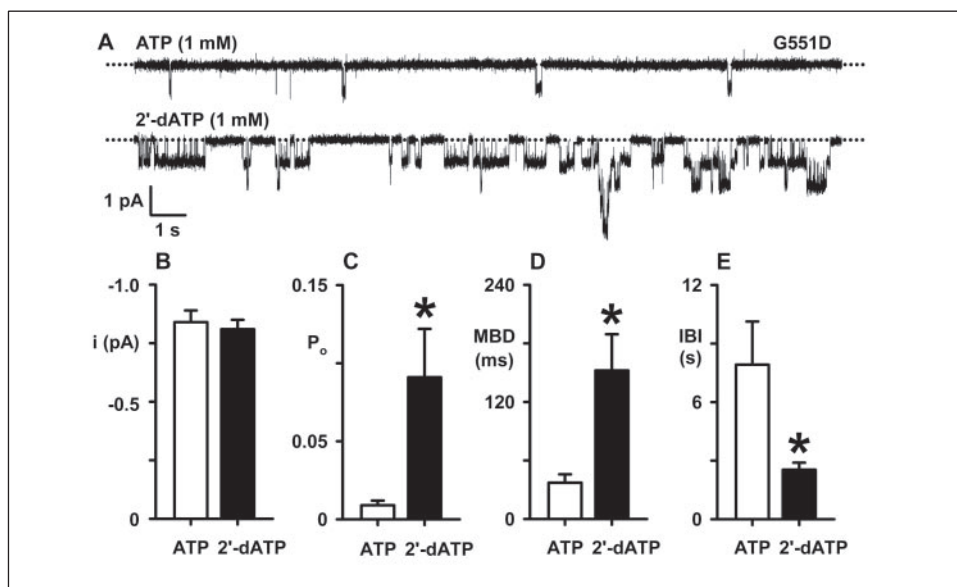

FIGURE 8. **G1349D-CFTR Cl⁻ channels are potentiated by 2'-dATP.** *A*, single-channel recordings of G1349D-CFTR in the presence of either ATP (1 mM) or 2'-dATP (1 mM). PKA (75 nM) was continuously present in the intracellular solution. *B–E*, effects of 2'-dATP on i, P_o, MBD, and IBI of G1349D-CFTR, respectively. *Columns* and *error bars* indicate means + S.E. ($n = 5$). The *asterisks* indicate values that are significantly different from the control values ($p < 0.05$).

reduced. Of note, using a molecular model of the NBD dimer, Moran *et al.* (15) demonstrated that G551D- and G1349D-CFTR each destabilize ATP binding to sites 1 and 2. Perhaps this global disruption of NBD dimer function explains why these mutants have such severe effects on CFTR activity.

Mechanisms of Action of CFTR Potentiators

Our results demonstrate that phloxine B and 2'-dATP have profound effects on the gating behavior of CF mutants. The effects of these agents are so striking that channels unobserved under control conditions appear to be "activated" in their presence. Below, we use the model of Vergani *et al.* (5) to discuss the effects of CFTR potentiators on wild-type, G551D-, and G1349D-CFTR.

Phloxine B—We previously demonstrated that saturating (micromolar) concentrations of phloxine B potentiate wild-type CFTR by slowing the rate of channel closure without altering the opening rate (11). Re-examining these effects of phloxine B on wild-type CFTR using the model of Vergani *et al.* (5), we suggest that the interaction of phloxine B

with the NBDs might strengthen the binding energy for stable dimer formation, and thus, prolong the interaction of ATP with site 2. Consistent with this idea, phloxine B prolonged the MBD of G551D-CFTR (present study). However, phloxine B also decreased the IBI of G551D- and G1349D-CFTR (present study), suggesting that the drug can promote NBD dimer formation for some, but not other, CF mutants (*e.g.* ΔF508 (11)).

Our present results supported the idea that phloxine B interacts directly with NBD2 to potentiate CFTR channel gating. G1349D-CFTR abolished the phloxine B-induced prolongation of channel openings, suggesting that G1349 either directly or indirectly contributes to the binding site for phloxine B. However, because phloxine B did not potentiate the CFTR Cl⁻ channel in the absence of ATP (11), we consider it unlikely that phloxine B interacts directly with site 1. Instead, the phloxine B-binding site might be located at the interface of NBD1 and NBD2 based on the interaction of CFTR potentiators with a molecular model of the NBD dimer (15). The interaction of phloxine B with this site might, via a steric effect on the conformation of the NBDs, enhance the affinity of ATP binding, and thus,

the stability of the NBD dimer. Of note, this mechanism of action is similar to that proposed by Ai *et al.* (32) to explain how capsaicin and genistein potentiate the CFTR Cl⁻ channel.

PP$_i$—Gunderson and Kopito (12) and Carson et al. (13) demonstrated that PP$_i$ potentiates robustly wild-type CFTR by accelerating the rate of channel opening and slowing dramatically the rate of channel closure. Using the model of Vergani *et al.* (5), we suggest that PP$_i$ interacts with the NBD dimer at site 2 to disrupt the hydrolysis of ATP that determines the duration of channel openings. Consistent with this idea, G551D-CFTR markedly attenuated PP$_i$ potentiation of CFTR. Moreover, G1349D-CFTR abolished the potentiation of CFTR Cl⁻ currents by PP$_i$, suggesting that PP$_i$ might also bind to site 1 and accelerate channel opening by providing binding energy to drive NBD dimerization. However, because PP$_i$ cannot substitute for ATP in supporting CFTR channel gating (13) and because G1349D-CFTR has global effects on NBD dimer function (15), we suggest that the interaction of PP$_i$ with site 2 might energize NBD dimerization.

2′-dATP—Like PP$_i$ (13), 2′-dATP augments wild-type CFTR channel gating by accelerating the rate of channel opening and slowing the closing rate (Ref. 14 and present study). Because 2′-dATP alone can open the CFTR Cl⁻ channel and because it can substitute for ATP in supporting channel activity (Ref. 14 and present study), we propose that 2′-dATP can interact with both sites 1 and 2. Moreover, to explain the faster rate of channel opening in the presence of 2′-dATP (Ref. 14 and present study), we suggest that the tighter binding of 2′-dATP to sites 1 and 2 drives NBD dimerization. Similarly, a slower rate of 2′-dATP hydrolysis when compared with that of ATP might account for the prolongation of channel openings in the presence of 2′-dATP (Ref. 14 and present study).

Our studies of 2′-dATP are significant in two respects. First, among the agents that we tested, only 2′-dATP potentiated the gating behavior of both G551D- and G1349D-CFTR. We speculate that the reason why 2′-dATP rescued G1349D-CFTR channel gating, whereas phloxine B and PP$_i$ did not, is that 2′-dATP binds tightly to both sites 1 and 2.

Second, 2′-dATP prolonged the MBD of G551D-CFTR to a magnitude equivalent to that of wild-type CFTR in the presence of ATP. However, 2′-dATP only attenuated partially the extended IBI of G551D-CFTR. (Note that phloxine B had similar effects on G551D-CFTR). These data indicate that for G551D-CFTR, the defect in channel closing is easier to rescue than that of channel opening. An explanation for the effects of 2′-dATP on G551D-CFTR channel gating is provided by the $C_1 \leftrightarrow C_2 \leftrightarrow O$ model of CFTR channel gating (30). In this model, the largest energy barrier is the transition from the long duration closed state (C_1) to the bursting state ($C_2 \leftrightarrow O$). Given that the IBI of G551D-CFTR is 45-fold longer than that of wild-type CFTR (Fig. 1*E*), the energy barrier opposing the opening of the G551D-CFTR Cl⁻ channel must be considerably greater than that of wild-type CFTR. Thus, although 2′-dATP and phloxine B might provide sufficient energy to G551D-CFTR to normalize the rate of channel closing, this energy is insufficient to rescue the defect in channel opening. Clearly, future studies will need to address the relationship between the binding energy and efficacy of CFTR potentiators.

To summarize, we propose that phloxine B interacts with a site distinct from the ATP-binding sites of CFTR to prolong the interaction of ATP with site 2, and thus, the duration of channel openings. PP$_i$ competes with ATP for interaction with site 2. When PP$_i$ binds to site 2, it increased the frequency and duration of channel openings by energizing NBD dimerization and blocking ATP hydrolysis. 2′-dATP binds tightly to sites 1 and 2 to drive NBD dimerization. Moreover, because 2′-dATP is hydrolyzed more slowly than ATP, the duration of channel openings are prolonged. Thus, phloxine B, PP$_i$ and 2′-dATP enhanced CFTR channel gating by distinct mechanisms.

REFERENCES

1. Riordan, J. R., Rommens, J. M., Kerem, B.-S., Alon, N., Rozmahel, R., Grzelczak, Z., Zielenski, J., Lok, S., Plavsic, N., Chou, J.-L., Drumm, M. L., Iannuzzi, M. C., Collins, F. S., and Tsui, L.-C. (1989) *Science* **245,** 1066–1073
2. Welsh, M. J., Ramsey, B. W., Accurso, F., and Cutting, G. R. (2001) in *The Metabolic and Molecular Basis of Inherited Disease* (Scriver, C. R., Beaudet, A. L., Sly, W. S., and Valle, D., eds) pp. 5121–5188, McGraw-Hill Inc., New York
3. Sheppard, D. N., and Welsh, M. J. (1999) *Physiol. Rev.* **79,** S23-S45
4. Lewis, H. A., Buchanan, S. G., Burley, S. K., Conners, K., Dickey, M., Dorwart, M., Fowler, R., Gao, X., Guggino, W. B., Hendrickson, W. A., Hunt, J. F., Kearins, M. C., Lorimer, D., Maloney, P. C., Post, K. W., Rajashankar, K. R., Rutter, M. E., Sauder, J. M., Shriver, S., Thibodeau, P. H., Thomas, P. J., Zhang, M., Zhao, X., and Emtage, S. (2004) *EMBO J.* **23,** 282–293
5. Vergani, P., Lockless, S. W., Nairn, A. C., and Gadsby, D. C. (2005) *Nature* **433,** 876–880
6. Riordan, J. R. (2005) *Annu. Rev. Physiol.* **67,** 701–718
7. Ostedgaard, L. S., Baldursson, O., Vermeer, D. W., Welsh, M. J., and Robertson, A. D. (2000) *Proc. Natl. Acad. Sci. U. S. A.* **97,** 5657–5662
8. Sullivan, L. P., Wallace, D. P., and Grantham, J. J. (1998) *J. Am. Soc. Nephrol.* **9,** 903–916
9. Gabriel, S. E., Brigman, K. N., Koller, B. H., Boucher, R. C., and Stutts, M. J. (1994) *Science* **266,** 107–109
10. Sheppard, D. N. (2004) *J. Gen. Physiol.* **124,** 109–113
11. Cai, Z., and Sheppard, D. N. (2002) *J. Biol. Chem.* **277,** 19546–19553
12. Gunderson, K. L., and Kopito, R. R. (1994) *J. Biol. Chem.* **269,** 19349–19353
13. Carson, M. R., Winter, M. C., Travis, S. M., and Welsh, M. J. (1995) *J. Biol. Chem.* **270,** 20466–20472
14. Aleksandrov, A. A., Aleksandrov, L., and Riordan, J. R. (2002) *FEBS Lett.* **518,** 183–188
15. Moran, O., Galietta, L. J. V., and Zegarra-Moran, O. (2005) *CMLS Cell. Mol. Life Sci.* **62,** 446–460
16. Callebaut, I., Eudes, R., Mornon, J.-P., and Lehn, P. (2004) *CMLS Cell. Mol. Life Sci.* **61,** 230–242
17. Anderson, M. P., and Welsh, M. J. (1992) *Science* **257,** 1701–1704
18. Smit, L. S., Wilkinson, D. J., Mansoura, M. K., Collins, F. S., and Dawson, D. C. (1993) *Proc. Natl. Acad. Sci. U. S. A.* **90,** 9963–9967
19. Li, C., Ramjeesingh, M., Wang, W., Garami, E., Hewryk, M., Lee, D., Rommens, J. M., Galley, K., and Bear, C. E. (1996) *J. Biol. Chem.* **271,** 28463–28468
20. Vergani, P., Nairn, A. C., and Gadsby, D. C. (2003) *J. Gen. Physiol.* **120,** 17–36
21. Sheppard, D. N., and Robinson, K. A. (1997) *J. Physiol.* (*Lond.*) **503,** 333–346
22. Zegarra-Moran, O., Romio, L., Folli, C., Caci, E., Becq, F., Vierfond, J.-M., Mettey, Y., Cabrini, G., Fanen, P., and Galietta, L. J. V. (2002) *Br. J. Pharmacol.* **137,** 504–512
23. Hamill, O. P., Marty, A., Neher, E., Sakmann, B., and Sigworth, F. J. (1981) *Pfluegers Arch. Eur. J. Physiol.* **391,** 85–100
24. Venglarik, C. J., Schultz, B. D., Frizzell, R. A., and Bridges, R. J. (1994) *J. Gen. Physiol.* **104,** 123–146
25. Lansdell, K. A., Delaney, S. J., Lunn, D. P., Thomson, S. A., Sheppard, D. N., and Wainwright, B. J. (1998) *J. Physiol.* (*Lond.*) **508,** 379–392
26. Lansdell, K. A., Cai, Z., Kidd, J. F., and Sheppard, D. N. (2000) *J. Physiol.* (*Lond.*) **524,** 317–330
27. Carson, M. R., Travis, S. M., and Welsh, M. J. (1995) *J. Biol. Chem.* **270,** 1711–1717
28. Cai, Z., Scott-Ward, T. S., and Sheppard, D. N. (2003) *J. Gen. Physiol.* **122,** 605–620
29. Qin, F., and Li, L. (2004) *Biophys. J.* **87,** 1657–1671
30. Winter, M. C., Sheppard, D. N., Carson, M. R., and Welsh, M. J. (1994) *Biophys. J.* **66,** 1398–1403
31. Logan, J., Hiestand, D., Daram, P., Huang, Z., Muccio, D. D., Hartman, J., Haley, B., Cook, W. J., and Sorscher, E. J. (1994) *J. Clin. Investig.* **94,** 228–236
32. Ai, T., Bompadre, S. G., Wang, X., Hu, S., Li, M., and Hwang, T.-C. (2004) *Mol. Pharmacol.* **65,** 1415–1426

Differential Sensitivity of the Cystic Fibrosis (CF)-associated Mutants G551D and G1349D to Potentiators of the Cystic Fibrosis Transmembrane Conductance Regulator (CFTR) Cl⁻ Channel

Zhiwei Cai, Alessandro Taddei and David N. Sheppard

Access the most updated version of this article at doi: 10.1074/jbc.M510576200

Alerts:
- When this article is cited
- When a correction for this article is posted

Click here to choose from all of JBC's e-mail alerts

This article cites 31 references, 15 of which can be accessed free at
http://www.jbc.org/content/281/4/1970.full.html#ref-list-1